Stem Cell Reports
Article

ISSCR

OPEN ACCESS

Programming of neural progenitors of the adult subependymal zone towards a glutamatergic neuron lineage by neurogenin 2

Sophie Péron,[1,2,15] Leo M. Miyakoshi,[3,14,15] Monika S. Brill,[4,5,15] Diana Manzano-Franco,[6] Julia Serrano-López,[7,8,9] Wenqiang Fan,[1] Nicolás Marichal,[2] Alexander Ghanem,[10] Karl-Klaus Conzelmann,[10] Marisa Karow,[11] Felipe Ortega,[7,8,9] Sergio Gascón,[6,16,*] and Benedikt Berninger[1,2,12,13,16,*]

[1]Research Group "Adult Neurogenesis and Cellular Reprogramming", Institute of Physiological Chemistry, University Medical Center Johannes Gutenberg University, Mainz, Germany
[2]Centre for Developmental Neurobiology, Institute of Psychiatry, Psychology & Neuroscience, King's College London, London, UK
[3]Physiological Genomics, Institute of Physiology, Ludwig-Maximilians University Munich, Munich, Germany
[4]Institute of Neuronal Cell Biology, Technical University Munich, Munich, Germany
[5]Munich Cluster of Systems Neurology (SyNergy), Munich, Germany
[6]Department of Molecular, Cellular and Developmental Neurobiology, Cajal Institute – CSIC, Madrid, Spain
[7]Department of Biochemistry and Molecular Biology, Faculty of Veterinary, Universidad Complutense de Madrid (UCM), Madrid, Spain
[8]Instituto Universitario de Investigación en Neuroquímica (IUIN), Madrid, Spain
[9]Instituto de Investigación Sanitaria San Carlos (IdISSC), Madrid, Spain
[10]Max von Pettenkofer Institute and Gene Center, Ludwig Maximilians-University Munich, Munich, Germany
[11]Institute of Biochemistry, Friedrich-Alexander Universität Nürnberg-Erlangen, Erlangen, Germany
[12]MRC Centre for Neurodevelopmental Disorders, Institute of Psychiatry, Psychology & Neuroscience, King's College London, London, UK
[13]Focus Program Translational Neurosciences, Johannes Gutenberg University, Mainz, Germany
[14]Present address: Institut Pasteur de Lille, Lille, France
[15]These authors contributed equally
[16]Senior authors
*Correspondence: sgascon@cajal.csic.es (S.G.), benedikt.berninger@kcl.ac.uk (B.B.)
https://doi.org/10.1016/j.stemcr.2023.10.019

SUMMARY

Although adult subependymal zone (SEZ) neural stem cells mostly generate GABAergic interneurons, a small progenitor population expresses the proneural gene *Neurog2* and produces glutamatergic neurons. Here, we determined whether *Neurog2* could respecify SEZ neural stem cells and their progeny toward a glutamatergic fate. Retrovirus-mediated expression of *Neurog2* induced the glutamatergic lineage markers TBR2 and TBR1 in cultured SEZ progenitors, which differentiated into functional glutamatergic neurons. Likewise, *Neurog2*-transduced SEZ progenitors acquired glutamatergic neuron hallmarks *in vivo*. Intriguingly, they failed to migrate toward the olfactory bulb and instead differentiated within the SEZ or the adjacent striatum, where they received connections from local neurons, as indicated by rabies virus-mediated monosynaptic tracing. In contrast, lentivirus-mediated expression of *Neurog2* failed to reprogram early SEZ neurons, which maintained GABAergic identity and migrated to the olfactory bulb. Our data show that NEUROG2 can program SEZ progenitors toward a glutamatergic identity but fails to reprogram their neuronal progeny.

INTRODUCTION

Accruing evidence indicates that neural stem cells (NSCs) lining the walls of the lateral ventricle in the postnatal and adult subependymal zone (SEZ) exhibit regional identity, thereby conferring fate restrictions on NSCs (Obernier and Alvarez-Buylla, 2019). Because of this characteristic mosaic organization of the SEZ, NSCs residing in different SEZ domains along the rostro-caudal and dorsal-ventral axes generate neurons of distinct subtype identities and become subsequently destined for distinct sub-domains within the olfactory bulb (OB) (Azim et al., 2015; Brill et al., 2009; Cebrian Silla et al., 2021; Merkle et al., 2007; Sequerra, 2014). Grafting experiments indicate that these region-specific identities do not become erased upon placing NSCs into heterotopic locations, suggesting that extrinsic signals provided locally are not sufficient to reprogram the intrinsic fate restrictions of NSCs (Merkle et al., 2007). Furthermore, regional fate restrictions appear to extend even to the decision between neuronal and glial fates, as indicated by the fact that oligodendrogliogenic NSCs are enriched in the dorsal and septal SEZ and may constitute a lineage distinct from neurogenic NSCs (Delgado et al., 2021; Llorens-Bobadilla et al., 2015; Mizrak et al., 2019; Ortega et al., 2013).

Although the majority of NSCs from the adult SEZ give rise to several types of GABAergic or tyrosine hydroxylase-expressing interneurons (Lim and Alvarez-Buylla, 2014), previous work has shown that a small subpopulation of NSCs located in the dorsal SEZ can generate juxtaglomerular glutamatergic neurons (Brill et al., 2009). This subpopulation is characterized by sequential expression of PAX6, NEUROG2, TBR2, and TBR1 (Brill et al., 2009) that characterizes glutamatergic neuron producing lineages throughout the forebrain (Hevner et al., 2006). Forced transcription factor expression can alter fate restrictions of neural cells beyond the stem cell stage (Arlotta and Berninger, 2014; Rouaux and Arlotta, 2013). Forced expression

of *Pax6* (Hack et al., 2005), *Dlx2* (Brill et al., 2008), and *Fezf2* (Zuccotti et al., 2014) has been shown to shift subtype specification within the adult SEZ *in vivo*. When cultured under neurosphere conditions (high concentrations of epidermal growth factor [EGF] and fibroblast growth factor-2 [FGF2]), adult SEZ stem and progenitor cells could be directed toward generation of fully functional glutamatergic neurons by retrovirus-mediated expression of *Neurog2* (Berninger et al., 2007b). Moreover, upon transplantation into the adult hippocampal dentate gyrus, *Neurog2*-expressing adult SEZ stem or progenitor cells exhibited morphological similarities to endogenous dentate granule neurons and some degree of functional integration (Chen et al., 2012). However, exposure to EGF and FGF2 exerts dramatic effects on NSCs that may include a partial loss of regional specification (Gabay et al., 2003; Hack et al., 2004) and may render these cells more permissive to NEUROG2. Thus, in the present study, we addressed the question of whether NEUROG2 can overcome fate restrictions of adult SEZ stem and progenitor cells in the absence of elevated growth factor signaling and drive these toward the acquisition of a glutamatergic phenotype and, if so, whether such effect would extend into the life of adult-generated SEZ-derived neuroblasts and postmitotic neurons.

RESULTS

NEUROG2 activates forebrain glutamatergic neurogenesis in SEZ progenitors but fails to do so in young postmitotic neurons

Given that adult-generated glutamatergic OB neurons originate from progenitors located in the dorsal part of the SEZ that express NEUROG2 (Brill et al., 2009), we wondered whether ectopic expression of this transcription factor could program progenitors from the ventral SEZ, which otherwise give rise almost exclusively to GABAergic interneurons, toward a glutamatergic neuron identity. To address this question we took advantage of an adherent culture of the adult SEZ (Costa et al., 2011; Ortega et al., 2011), which preserves the ratio of GABAergic and glutamatergic neurogenesis as observed *in vivo* (Brill et al., 2009), and transduced proliferating progenitors with a retrovirus encoding *Neurog2*, followed by the reporter *dsRed* behind an internal ribosomal entry site (IRES) (RV-CAG-*Neurog2*-IRES-*dsRed*) or, alternatively, with a control retroviral vector encoding only *dsRed* after the IRES (RV-CAG-IRES-*dsRed*) (Figure 1A). We first investigated whether *Neurog2* expression would trigger morphological changes in the SEZ-derived neurons that might reflect a change in neuronal subtype identity (Figures 1 and S1). We observed that the TUBB3-positive neurons expressing *Neurog2* exhibited a more complex arborization than the control cells already at 5 days post-transduction (DPT), as indicated by a larger number of Sholl intersections of traced processes (Figures S1A and S1C). At 9 DPT, the neurons derived from the *Neurog2*-transduced cells still displayed more complex arbors and markedly increased the length of the processes, compared with control-transduced cells (Figures 1B–1E, S1B, and S1C). Moreover, plotting neurite length versus the number of intersections revealed that the *Neurog2*-transduced cell population distinctly segregated from the control-transduced counterparts (Figure 1F), suggesting that NEUROG2 instructs differentiation of SEZ progenitors toward a neuronal subtype morphologically distinct from the non-manipulated neuronal SEZ lineages. At a later stage of 12 DPT, both control and *Neurog2*-transduced cells showed a plateau or a slight decrease in neurite length and complexity (Figures S1A–S1C), but the differences in morphological complexity between the control and *Neurog2*-transduced cells persisted.

Given NEUROG2's well-established role in driving forebrain progenitors toward a glutamatergic neuron identity (Dennis et al., 2019; Fode et al., 2000; Kovach et al., 2013), we next studied whether forced *Neurog2* expression induced hallmarks of glutamatergic neurogenesis such as the sequential expression of the transcription factors TBR2 and TBR1 (Hevner et al., 2006). Indeed, at 7 DPT, TBR2 was expressed in a subpopulation of *Neurog2*-transduced cells (44% ± 7%; Figures 2A and 2D). At 5 DPT, TBR1 was detected in few cells (7% ± 9%) (Figure S2A), while at 9 DPT, it was expressed by the majority (62% ± 5%; Figures 2A, 2D, and S2A), slightly decreasing by 12 DPT (50% ± 9%; Figure S2A). Both transcription factors were scarcely detected in controls (3% ± 1% for TBR2 and 3% ± 3% for TBR1) (Figures 2D and S2A–S2C). Consistent with a change toward a glutamatergic neuron identity, *Neurog2*-transduced neurons were mostly negative for the neurotransmitter γ-aminobutyric acid (GABA), in contrast to control virus-transduced cells (RV-*Neurog2*, 13% ± 7%; RV-control, 80% ± 14%; Figures 2C, 2D, and S2C). Finally, in long-term cultures of *Neurog2*-transduced cells we detected abundant expression of the vesicular glutamate transporter 1 (VGlut1), which was virtually absent in control cultures, as previously reported (Brill et al., 2009) (Figure S2D). Likewise, patch-clamp recordings in these long-term cultures showed that, while control cells mostly formed functional GABAergic synapses, as reported previously (Brill et al., 2009; Costa et al., 2011), *Neurog2*-expressing neurons gave rise to glutamatergic transmission as illustrated by the pair-recording shown in Figure S2E (n = 6 pairs analyzed).

In the above experiments, use of retroviral vectors encoding *Neurog2* restricted transduction to dividing cells, most of which are transit-amplifying precursors (TAP) (Costa et al., 2011; Doetsch et al., 2002). We next asked whether

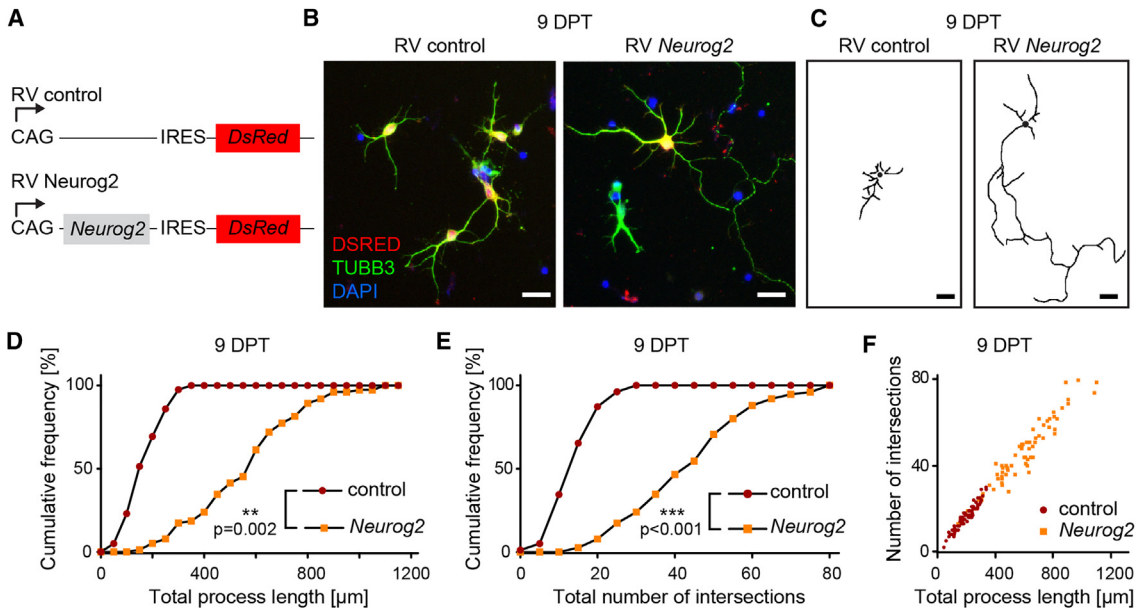

Figure 1. Neurons derived from SEZ progenitors transduced with a *Neurog2*-encoding retroviral vector develop more complex morphologies

(A) Scheme of the retroviral vectors (RV) CAG-*Neurog2*-IRES-*dsRed* and control CAG-IRES-*dsRed*.

(B) Micrographs depict TUBB3-positive neurons derived from SEZ progenitors that had been transduced 9 days earlier with the control or *Neurog2*-encoding retrovirus.

(C) Pictures are examples of neuronal processes traced in neurons from (B).

(D–F) Graphs show the total number of intersections and process length as determined by Sholl analysis in control- and *Neurog2*-transduced neurons. Note that the expression of *Neurog2* increased the length and number of intersections.

Error bars indicate mean ± SD, 75–78 neurons/group from 3 independent cultures, Kolmogorov-Smirnov test (D and E). Scale bars: 20 µm (B and C). See also Figure S1.

induction of a glutamatergic program would be possible at later stages of lineage progression (i.e., after the last cell division when these cells become postmitotic and commence differentiation). Thus, we used lentiviral vectors, which transduce both dividing and non-dividing cells, encoding either *Neurog2* and *eGfp* (LV-hSyn-*Neurog2*-IRES-*eGfp*) or *eGfp* reporter alone as control (LV-hSyn-IRES-*eGfp*). In these constructs, the expression of *Neurog2* and the reporter are driven by the minimal human synapsin promoter (hSyn; Figure S3A), which is transcriptionally active only in postmitotic neurons (Gascon et al., 2008). Accordingly, transduction of primary cortical cultures using either construct led to efficient expression of *eGfp* restricted to TUBB3-immunoreactive neurons (Figures S3B and S3C) while transduction with LV-hSyn-*Neurog2*-IRES-*eGfp* resulted in efficient expression of NEUROG2 in eGFP$^+$/TUBB3$^+$ neurons (Figure S3C). We next transduced adult SEZ cultures with these lentiviruses. Contrary to the effect mediated by retroviral expression of *Neurog2* at the progenitor stage, lentiviral expression of *Neurog2* in immature postmitotic neurons did not induce TBR2 (4% ± 6%) or TBR1 (1% ± 2%) (Figures 2B and 2D). Indeed, the percentage of cells positive for TBR2 and/or TBR1 in LV-hSyn-*Neurog2*-IRES-*eGfp*-transduced cultures was comparable with LV-hSyn-IRES-*eGfp* controls (1 ± 1% for TBR2 and 3% ± 3% for TBR1) (Figures 2D, S2B, and S2C). In agreement with the failure of NEUROG2 to activate a glutamatergic program in postmitotic neurons (Figures 2B–2D, and S3D), cells transduced with LV-hSyn-*Neurog2*-IRES-*eGfp* maintained GABA immunoreactivity (LV-*Neurog2*, 90% ± 9%; LV-control, 81% ± 18%; Figures 2C and 2D; see controls in Figure S2C).

Together, these data indicate SEZ progenitors targeted by *Neurog2*-encoding retrovirus undergo fate conversion whereas targeting their postmitotic progeny with a *Neurog2*-encoding lentivirus fails inducing glutamatergic lineage progression.

NEUROG2-mediated fate conversion of adult NSC progeny *in vivo*

Next, we investigated the effects of forced *Neurog2* expression in actively dividing adult SEZ progenitors *in vivo*. To this end, we stereotactically injected retroviruses encoding *dsRed* or *Neurog2*-IRES-*dsRed* into the adult SEZ. At 2 DPT,

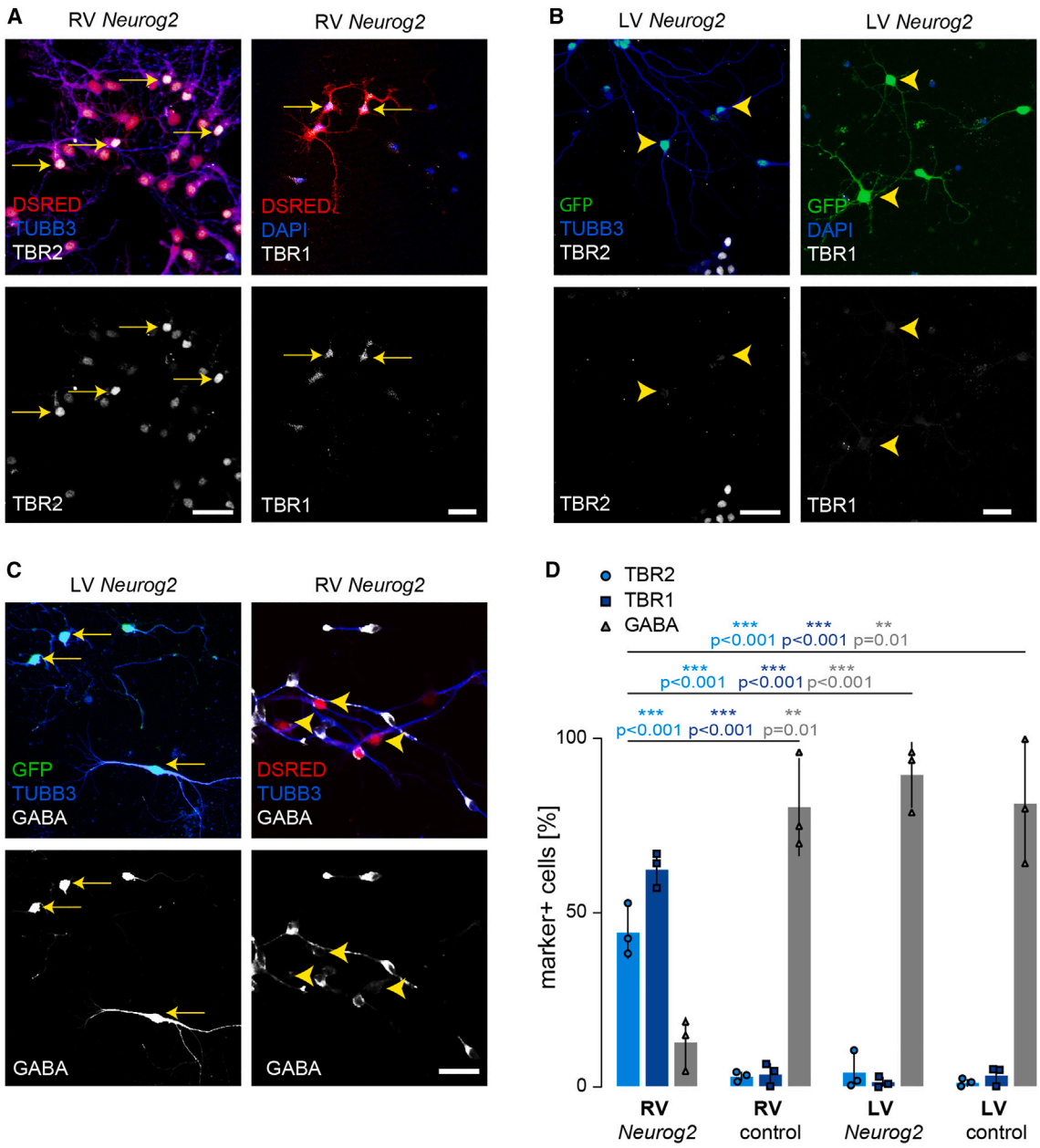

Figure 2. NEUROG2 induces glutamatergic neuron hallmarks when expressed in dividing progenitors but not in young postmitotic neurons

(A) Cells from primary SEZ cultures transduced with the RV-CAG-*Neurog2*-IRES-*dsRed* differentiate into TUBB3-positive neurons expressing TBR2 (arrows, left panel) at 7 DPT and TBR1 at 9 DPT (arrows, middle panel).

(B) Cells transduced with the lentiviral hSyn-*Neurog2*-IRES-*eGfp* vector fail to induce TBR2 (arrowheads, left panel) or TBR1 (arrowheads, right panel). Note the cluster of non-transduced progenitors expressing TBR2 occurring at low frequency in SEZ cultures.

(C) Cells in primary cultures of the SEZ transduced with the lentiviral hSyn-*Neurog2*-IRES-*eGfp* vector retain GABA immunoreactivity (left panel, arrows) at 7 DPT, while those that had been transduced with the retroviral CAG-*Neurog2*-IRES-*dsRed* do not express GABA (right panel, arrowheads).

(D) Histogram showing the proportion of transduced cells that were immunoreactive for TBR2, TBR1, or GABA following transduction with control or *Neurog2*-encoding retroviruses and lentiviruses.

Error bars indicate mean ± SD, n = 3 independent experiments. One-way ANOVA followed by Tukey's honestly significant difference (HSD) post hoc test. Scale bars: 60 μm (A and C). See also Figures S1 and S2. See also Figure S2.

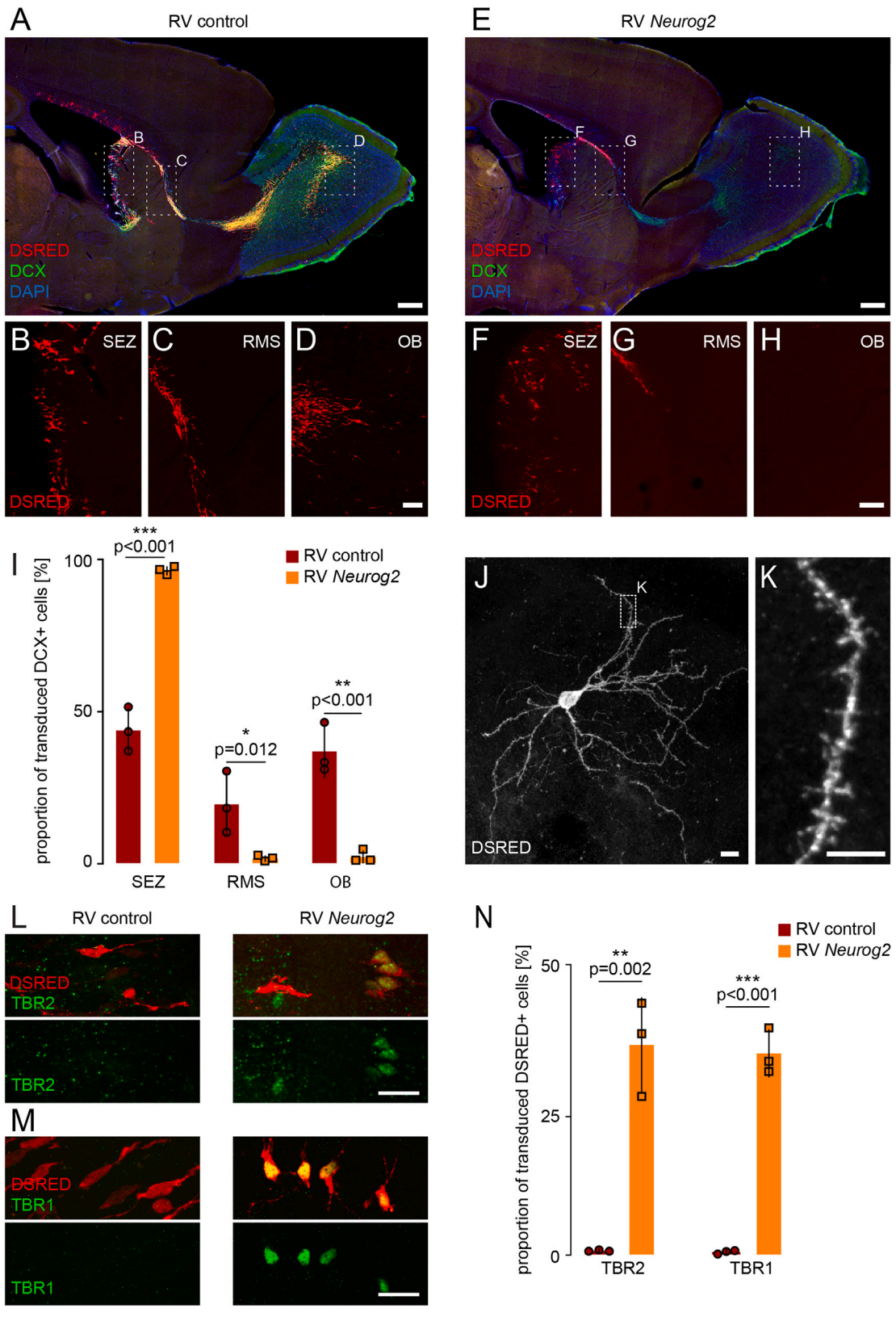

(legend on next page)

we observed no differences in the dorsoventral distribution of RFP$^+$ cells between the two cohorts (as shown in Figures S4A and S4B), indicating that the two viruses did not exhibit unexpected differential tropism toward specific SEZ subregions. Likewise, there were no differences in the cell types transduced by these viruses, primarily consisting of glial fibrillary acidic protein (GFAP)-negative/immature neuron marker doublecortin (DCX)-negative or GFAP-negative/DCX-positive cells (Figures S4C and S4D), corresponding to TAP and their resulting neuroblast progeny. A minority of cells were GFAP$^+$, indicating that a small number of self-renewing NSCs (Doetsch et al., 1999), or proliferating parenchymal astrocytes (Garcia et al., 2004) (see histogram in Figure S4D) had been transduced. Neither microglial (CD45$^+$) nor oligodendroglial (NG2$^+$) cells were identified in brains injected with either control or *Neurog2*-encoding viruses. By 7 DPT, there were also no significant differences in terms of dorsoventral distribution of the RFP$^+$ cells (Figures S4E and S4F). However, at this time point, RV-CAG-IRES-*dsRed*-transduced cells revealed the expected picture of retrovirally labeled cells chain-migrating along the entire extent of the rostral migratory stream (RMS) toward the core of the OB (Lois et al., 1996) (44% ± 7% of cells were found in the SEZ, 19% ± 10% of cells were migrating in the RMS, and 37% ± 9% of cells had reached the OB; n = 3 mice, 10,197 cells analyzed) (Figures 3A–3D and 3I). Following transduction with RV-CAG-*Neurog2*-IRES-*dsRed*, the proportion of transduced cells immunoreactive for DCX remained unchanged (Figure S5). However, in sharp contrast to control-transduced cells, *Neurog2*-expressing progenitors exhibited a drastically altered migratory behavior, abandoning chain migration (2% ± 1% of cells in the RMS; n = 3 mice, 823 cells analyzed) (Figures 3E–3I). Consequently, only very few cells reached the OB (2% ± 2%) (Figures 3E, 3H, and 3I), while most of them remained in the SEZ or entered the adjacent striatum (96% ± 1%) (Figures 3E, 3F, and 3I). In some cases, *Neurog2*-expressing cells differentiated into neurons with a dendritic arborization exhibiting dendritic spines (Figures 3J and 3K). This pattern of differentiation was not observed upon injection of control virus. To assess whether *Neurog2*-transduced cells acquire a glutamatergic neuron identity *in vivo*, we immunostained for TBR2 and TBR1. Virtually no Tbr2-positive cells were detected in controls in the ventral SEZ (0.7% ± 0.3% of control-transduced cells; 7 DPT, n = 3 mice, 962 cells analyzed). In sharp contrast, 36% ± 8% of *Neurog2*-expressing cells were found to be TBR2 immunoreactive (7 DPT, n = 3 mice, 95 cells analyzed) (Figures 3L and 3N). Likewise, 35 ± 5% of *Neurog2*-transduced cells were TBR1 positive (7 DPT, n = 3 mice, 147 cells analyzed), while control-transduced cells were by and large TBR1 negative (0.5% ± 0.4%, 7 DPT, n = 3 mice, 333 cells analyzed) (Figures 3M and 3N). These data indicate that *Neurog2* expression is capable of enforcing a glutamatergic neuron program onto SEZ progenitors.

The fact that *Neurog2*-expressing neurons in the striatum displayed dendritic spines (Figure 3K), strongly suggested that these cells may serve as postsynaptic targets of striatal host circuit neurons. To further examine whether these neurons indeed receive presynaptic input within the striatum *in vivo*, we used rabies virus (RABV)-mediated transsynaptic tracing (Wickersham et al., 2007) to identify potential presynaptic partners. We first injected the retrovirus RV-*DsRedExpress2*-T2A-*G*-IRES-*TVA* together with the RV-*Neurog2*-IRES-*dsRed* into the SEZ, thereby conferring at the same time susceptibility to RABV transduction and capacity for transsynaptic spread (Bergami, 2015; Deshpande et al., 2013) while programming these cells toward the glutamatergic lineage. Eight days later, an EnvA-pseudotyped and glycoprotein G gene-deleted *eGfp*-expressing RABV was injected into the striatum, close to the SEZ, to target neurons potentially transduced with the two retroviruses

Figure 3. Retrovirus-mediated *Neurog2* expression alters the migration behavior of SEZ progenitors and induces their differentiation toward a glutamatergic fate *in vivo*

(A–D) Sagittal view of an adult mouse brain depicts cells transduced with the control RV-CAG-IRES-*dsRed* (red) (B) within the SEZ, migrating throughout the RMS (C), and reaching the OB (D).

(E–H) Micrographs show SEZ cells transduced with the RV-CAG-*Neurog2*-IRES-*dsRed* (red) in the areas corresponding to those in (A)–(D). Note that at 7 DPT, only few transduced neuroblasts entered the RMS (G). They failed to reach the core of the OB (H) and instead remained stationary in the anterior portion of the SEZ (F).

(I) Histogram showing the number of DCX-positive/dsRed-positive transduced cells in the SEZ, RMS, and OB at 7 DPT. Error bars indicate mean ± SD, n = 3/mice group, one-way ANOVA followed by Tukey's HSD post hoc test.

(J and K) Higher magnification images show a cell from (E)–(H), transduced with the RV-CAG-*Neurog2*-IRES-*dsRed*, which had acquired a pyramidal neuron-like morphology (J) with well-developed dendritic spines (K).

(L and M) Micrographs show expression of the transcription factors TBR2 (L) and TBR1 (M) (green) in SEZ cells transduced with retrovirus encoding *Neurog2* but not in cells transduced with the control retrovirus.

(N) Histogram showing the proportion of SEZ-derived neurons that express TBR2 and TBR1 following transduction with the control or the *Neurog2*-encoding retroviral vectors. Note that more than one-third of *Neurog2*-expressing cells up-regulated TBR2 and TBR1 at 7DPT. Error bars indicate mean ± SD, n = 3/mice group, t test. Scale bars: 1 mm (A and E), 100 μm (B–D and F–H), 20 μm (L and M), 10 μm (J), and 5 μm (K). See also Figures S4 and S5.

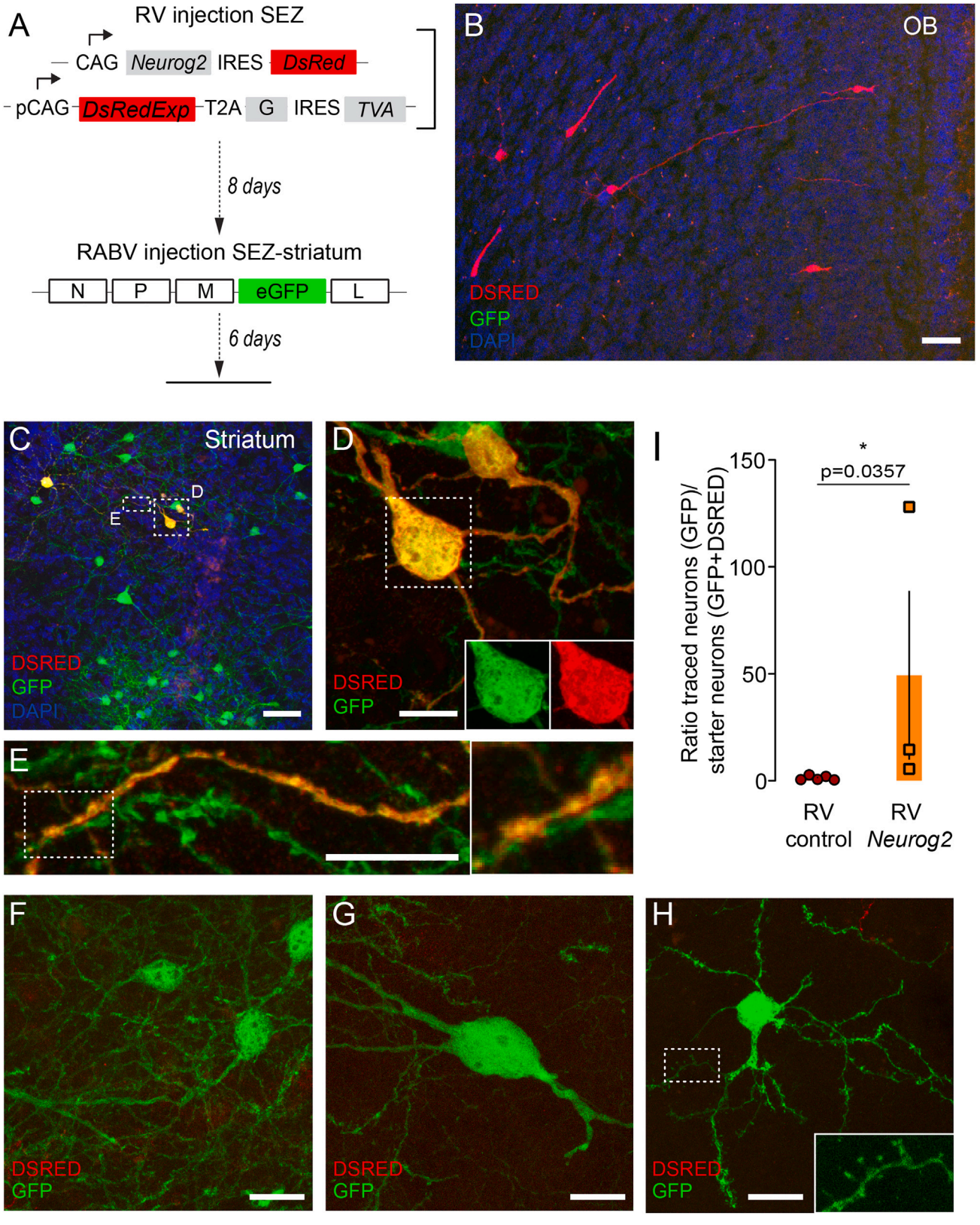

(legend on next page)

(i.e., expressing *TVA*, *G*, *Neurog2*, and *dsRed*) (Figure 4A). Six days later, as expected, cells that were presumably transduced only with RV-*DsRedExpress2*-T2A-*G*-IRES-*TVA* but not RV-*Neurog2*-IRES-*dsRed* had migrated by and large to the OB (Figure 4B). In sharp contrast, in the striatum we observed neurons that were both positive for dsRed and eGFP, suggesting that they were successfully transduced with both retroviruses as well as the RABV, thus serving as potential starter cells for transsynaptic RABV spread (Figures 4C–4E). Surrounding these putative starter cells, we found numerous eGFP-only-positive neurons of diverse sizes and morphologies, suggesting that different types of local striatal neurons acted as presynaptic partners of the SEZ-derived, *Neurog2*-programmed neurons (Figures 4C–4H). In particular, we observed many eGFP-only-positive neurons that exhibited morphologies of medium spiny neurons, characterized by numerous spines (Figure 4H). Overall, we observed a connectivity index of approximately 50 presynaptic cells versus putative starter cells (eGFP/eGFP+dsRed cells; Figure 4I). In contrast, only very few eGFP-positive cells were detected in the striatum of animals injected without the *Neurog2*-encoding retrovirus (Figures 4I and S6), demonstrating the requirement of NEUROG2-mediated programming of SEZ progenitors into striatum-resident neurons for successful tracing of presynaptic partners in the striatum.

The cellular responsiveness to NEUROG2 *in vivo* depends on prior lineage commitment

To assess whether NEUROG2 can still reprogram SEZ NSC progeny already committed to a GABAergic neuron fate toward the glutamatergic lineage *in vivo*, we next injected the LV-hSyn-*Neurog2*-IRES-*eGfp* vector into the adult SEZ (Figure 5). The presence of eGFP/DCX-double-positive cells leaving the SEZ and entering the RMS confirmed early-onset expression of the lentiviral construct *in vivo* (Figure 5A). However, lentivirus-driven expression of *Neurog2* did not induce aberrant migration, and most DCX-positive transduced cells reached the OB (LV-hSyn-IRES-*eGfp*: 9% ± 5% of cells in SEZ, 3% ± 0.6% of cells in RMS, and 88% ± 5% of cells in OB [n = 3 mice, 1,929 cells analyzed]; LV-hSyn-*Neurog2*-IRES-*eGfp*: 10% ± 4% of cells in SEZ, 3% ± 1% of cells in RMS, and 88% ± 6% of cells in OB [n = 3 mice, 855 cells analyzed]; Figure 5B). At 10 DPT, a large number of transduced cells were already present in the OB and dispersed radially toward more superficial layers, where they acquired the morphologies characteristic of GABAergic granule cells or periglomerular neurons (Figures 5C and 5D), and did not express the glutamatergic lineage markers TBR2 (Figures 5E and 5F) or TBR1 (Figures 5G and 5H). These results strongly suggest that *Neurog2* expression fails to alter the program of SEZ progeny *in vivo* once these have acquired neuronal identity. To assess potential biases due to variation in the expression levels caused by the respective use of retroviral or lentiviral vectors, we injected the RV-CAG-*Neurog2*-IRES-*dsRed* retrovirus directly into the RMS elbow instead of the SEZ (Figure 6A). This approach allowed targeting migrating neuroblasts that, while still dividing, were already committed to the neuronal lineage. In contrasts to injection of the same retrovirus into the SEZ proper, cells transduced in the RMS populated different layers of the OB (Figure 6B) and failed to activate TBR1 expression, either in the RMS (Figures 6E–6G) or the OB (Figures 6B–6D). However, we did observe a modest reduction in the number of *Neurog2*-transduced cells reaching the OB (Figure 6H). In conclusion, these experiments provide evidence that committed neuroblasts became refractory re-specification into glutamatergic neurons by NEUROG2, while their migratory behavior can still be compromised.

DISCUSSION

In the present study, we demonstrated that forced expression of *Neurog2* redirects the program of proliferating adult

Figure 4. Neurons derived from *Neurog2*-programmed SEZ progenitors are locally connected

(A) Experimental design of RABV-mediated connectivity tracing. CAG-*Neurog2*-IRES-*dsRed* retrovirus and pCAG-*DsRedExpress2*-T2A-G-IRES-*TVA* retrovirus were coninjected into the SEZ. Eight days later, an EnvA-pseudotyped and G gene-deleted *eGfp*-expressing RABV was injected in the vicinity of the injection site of the retroviruses, and analysis was performed 6 days later.

(B) DSRED-only-positive cells were detected in the OB, likely corresponding to cells transduced only with the pCAG-*DsRedExpress2*-T2A-G-IRES-*TVA* that had migrated normally to the OB.

(C and D) Upon NEUROG2 transduction, putative starter cells (yellow, expressing both dsRed and GFP) were found in the striatum, and first-order presynaptic partners (GFP only) could be traced locally.

(E) High-magnification micrographs depicting traced neurons forming physical contacts onto *Neurog2*-programmed neurons.

(F–H) Traced neurons exhibited various morphologies, many of which exhibited dendritic spines (inset in H).

(I) Histogram showing the proportion of GFP^+/GFP^++$dsRed^+$ neurons (connectivity index) found following control or *Neurog2* retrovirus injection into the SEZ.

Error bars indicate mean ± s.e.m., n = 3–5 mice/group, Mann-Whitney test. Scale bars: 100 μm (B), 50 μm (C), and 10 μm (D–H). See also Figure S6.

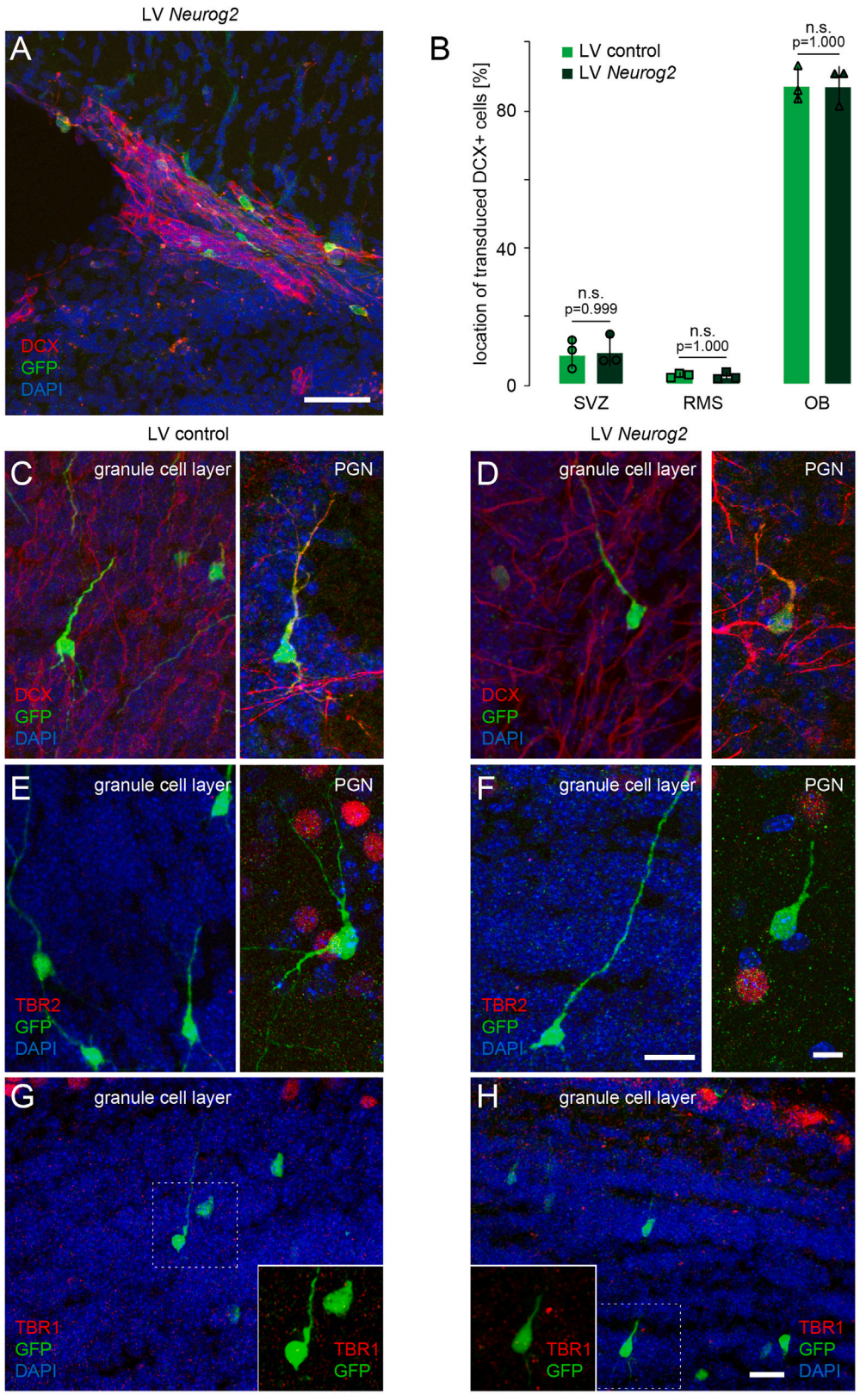

(legend on next page)

SEZ progenitors, normally giving rise to GABAergic OB neurons, toward generating neurons of the glutamatergic lineage. This indicates that NEUROG2 can override region-specific fate restrictions of adult NSCs. However, once SEZ-derived cells have differentiated into postmitotic neurons, NEUROG2 can no longer induce a lineage switch and neurons retain their GABAergic neuron identity. Thus, there appears to be a restricted window during lineage progression from NSC to neuron during which NEUROG2 can alter the program determining neuron class identity. Our data support the notion that competence to respond to NEUROG2 is cellular stage dependent. Likewise, a recent study has shown that early and late cortical progenitors (i.e., cells fated for different cortical laminar identities) respond differentially to NEUROG2 (Dennis et al., 2017).

Retroviruses predominantly transduce fast dividing progenitors both *in vitro* and *in vivo*. Thus, by using a retroviral vector for delivery of *Neurog2*, expression of the proneural gene was presumably confined to activated NSCs and TAPs as well as neuroblasts still dividing in the RMS. We found that retrovirus-mediated *Neurog2* expression resulted in the acquisition of a glutamatergic neuron identity, as read out by TBR2 and TBR1 expression, only in those progenitors residing in the SEZ but not the RMS. Furthermore, in accordance with a fate switch *in vivo*, cells targeted within the SEZ no longer migrated to the OB, but instead differentiated within the SEZ or the adjacent striatum. Thus, part of the fate switch induced by *Neurog2* likely involves an alteration of the migratory program normally controlled by *Dlx2* (Brill et al., 2008). Of note, previous work had shown that SEZ cells can be redirected from their normal migration route toward other brain regions upon co-transduction with retroviruses encoding *Neurog2* and *Isl1* (Rogelius et al., 2008).

In sharp contrast to the effect of retrovirus-mediated *Neurog2* expression in SEZ progenitors, targeting *Neurog2* to postmitotic neurons by using a lentivirus driving transgene expression from the human synapsin promoter (Gascon et al., 2008), failed to alter the already ongoing program of OB interneuron differentiation. Lentivirus-transduced cells continued migrating along the RMS to the OB where they took position within the granule cell layer and periglomerular layer for which most of the adult-generated neurons in the SEZ are destined (Merkle et al., 2007, 2014). Likewise, postmitotic expression of *Neurog2* did not cause overt changes in morphology as eGFP-positive cells exhibited morphologies reminiscent of OB interneurons.

Consistent with the *in vivo* data, primary cultures of neurons derived from SEZ progenitors were GABA immunoreactive following postmitotic *Neurog2* expression. Finally, postmitotic *Neurog2* expression failed to induce the expression of TBR2 and TBR1. In the absence of any evidence for a fate change, it thus appears that *Neurog2*-expressing SEZ-derived neurons maintain an interneuron identity normally acquired during lineage progression from NSC to neuron. These data suggest the establishment of powerful epigenetic barriers (Baumann et al., 2019) that impede a NEUROG2-instructed switch from a GABAergic to glutamatergic neuron identity. Interestingly, such barriers appear to be established prior to or at the neuroblast stage as injection of *Neurog2*-encoding retrovirus into the elbow of the RMS failed to cause re-specification toward a glutamatergic fate. However, the fact that migration toward the OB may still be compromised indicates that the gene expression programs guiding migratory behavior are still malleable under the influence of NEUROG2. These findings also suggest that the programming potency of NEUROG2 sharply declines when neurons start to migrate through the RMS and become postmitotic and is likely linked to the maturation of the neuronal epigenome during this transition, as indicated by the failure of upregulating TBR2, which is known to be a direct target of NEUROG2 (Kovach et al., 2013; Ochiai et al., 2009). Alternatively, or in addition to epigenetic barriers, the effectiveness of NEUROG2 action may be curtailed by signaling mechanisms regulating its phosphorylation state (Quan et al., 2016) or the formation of homo- versus heterodimers (Li et al., 2012). Also, dynamically regulated changes in

Figure 5. Expression of *Neurog2* fails to induce a glutamatergic phenotype in early neurons derived from the SEZ *in vivo*

(A) Micrograph shows early neurons (DCX, red) leaving the SEZ and expressing GFP (green), indicative of hSyn-promoter activity early during fate commitment.

(B) Quantification of the number of DCX-positive/GFP-positive lentivirus-transduced cells in the SEZ, RMS, and OB at 10 DPT. Note that expression of *Neurog2* in early neurons does not affect their migration to the OB. Error bars indicate mean ±SD, n = 3 mice/group, one-way ANOVA followed by Tukey's HSD post hoc test.

(C and D) Micrographs of the granule cell layer of the OB show lentivirus-transduced cells (green) migrating radially and integrating as granule and periglomerular neurons (PGN, insets, DCX red) at 10 DPT.

(E–H) Transduction of SEZ cells with either hSyn-*eGfp* control (in green) or hSyn-*Neurog2*-IRES-*eGfp* (in green) lentiviruses does not lead to the expression of TBR2 (in red) in granule neurons (E, F) or periglomerular neurons (PGN, insets), nor does it induce TBR1 expression in granule neurons (G, H).

Scale bars: 50 μm (B–F), 10 μm (insets in C–F), and 25 μm (G and H).

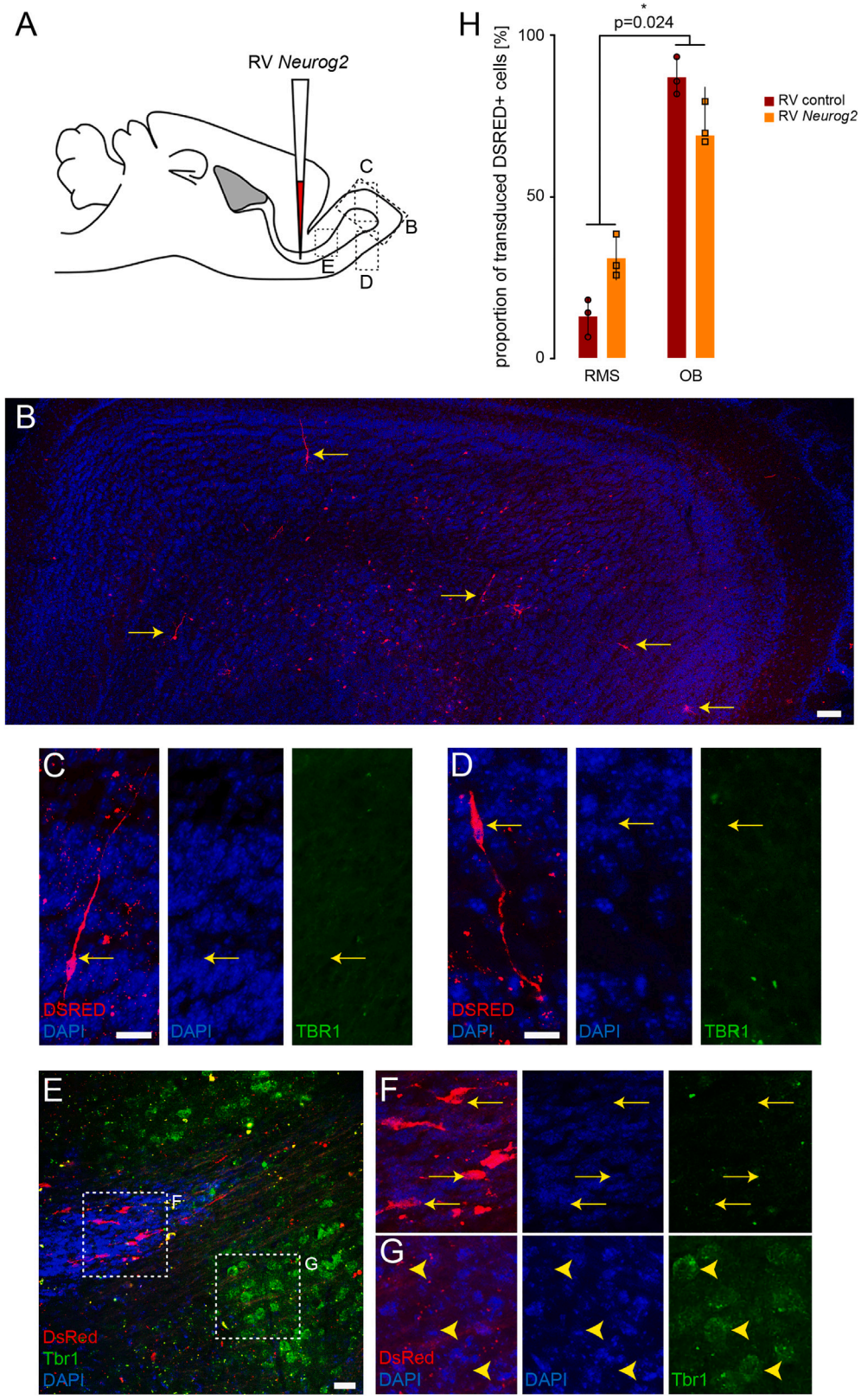

(legend on next page)

the level of protein synthesis during lineage progression by miRNAs (Baser et al., 2019) may render the competence of SEZ progenitors differentially susceptible to fate conversion. The failure of reprogramming at later stages of adult NSC lineage progression is even more intriguing given NEUROG2's capacity to induce TBR2 and TBR1 in early postnatal cortical astrocytes *in vitro* (Berninger et al., 2007a; Heinrich et al., 2010) and to reprogram glia into glutamatergic neurons *in vivo* (Felske et al., 2023; Gascon et al., 2016; Herrero-Navarro et al., 2021). The developmental window-specific actions of NEUROG2 on adult SEZ stem and progenitor cells exhibit remarkable parallelism as well as differences to that of the transcription factor FEZF2. FEZF2 was originally described as a transcription factor to specify the fate of cortical progenitors toward a corticofugal identity during development (Molyneaux et al., 2005). Subsequent work demonstrated that it can reprogram striatal progenitors toward a corticofugal identity *in vivo* (Rouaux and Arlotta, 2010), thus, causing not only a switch from GABAergic to glutamatergic neuron fate, but also eliciting a specific neuronal subtype conversion (from medium spiny neurons to corticofugal pyramidal neurons). Of note, FEZF2 reprogramming activity extends into early postmitotic life of a neuron but markedly declines in the course of few days (Rouaux and Arlotta, 2013), again suggesting the existence of a critical window of nuclear plasticity that closes with epigenetic changes that occur during neuronal maturation (Amamoto and Arlotta, 2014). Later, FEZF2 was found to program NSCs in the postnatal and adult SEZ toward a glutamatergic neuron identity (Zuccotti et al., 2014). In contrast to our findings when using NEUROG2, the FEZF2-induced fate switch was restricted specifically to the NSC stage but failed to convert both TAPs or dividing neuroblasts. Moreover, in contrast to the re-routing of *Neurog2*-expressing neurons reported here, progeny of *Fezf2*-expressing NSCs still migrated to the OB. Thus, cells of the adult SEZ NSC lineage exhibit differential competence to respond to FEZF2 or NEUROG2 along lineage progression.

Finally, RABV-mediated monosynaptic tracing indicates that the *Neurog2*-programmed neurons re-routed to the striatum received input from local neurons including medium spiny neurons. Future studies will be required to understand whether the integration of such non-canonical neurons provides functional excitatory input to the striatal circuitry, as it was the case in neurons derived from reprogrammed striatal astrocytes (Dorst et al., 2021), and if they could exert a meaningful modulatory effect on striatal circuit function. Be that as it may, our data provide evidence for remarkable plasticity within the lineage of adult NSCs. It will be interesting to learn whether this plasticity can be harnessed toward translational approaches to recruit adult NSC progeny for brain repair (Benraiss et al., 2013; Brill et al., 2009; Gage and Temple, 2013; Saghatelyan et al., 2004).

EXPERIMENTAL PROCEDURES

Resource availability

Corresponding authors

Further information and requests for resources and reagents should be directed to the corresponding authors, Sergio Gascón (sgascon@cajal.csic.es) or Benedikt Berninger (benedikt.berninger@kcl.ac.uk).

Materials availability

Materials can be requested from the corresponding authors.

Data and code availability

Data will be shared with the research community upon request.

Ethical approval

All animal procedures were performed in accordance with the guidelines of the German Animal Welfare Act and the European Directive 2010/63/EU for the protection of animals used for scientific purposes, and was approved by the state of Bavaria under license number 55.2-1-54-2531-144/07 or the state of Rhineland-Palatinate under license number 23 177 07-G-15-1-031.

SEZ primary culture

Following a previously established protocol by (Costa et al., 2011; Ortega et al., 2011), SEZ cultures were prepared from the lateral wall of the lateral ventricle of young adult (8–12 weeks) C57BL/6J mice (Costa et al., 2011; Ortega et al., 2011). Briefly, tissue was dissociated in 0.7 mg/mL hyaluronic acid (Sigma-Aldrich) and 1.33 mg/mL trypsin (Sigma-Aldrich) in Hank's balanced salt solution (HBSS; Invitrogen) with 2 mM glucose (Sigma-Aldrich) at 37°C for 30 min. After this enzymatic treatment, an equal volume

Figure 6. RMS-resident dividing neuroblasts are refractory to glutamatergic re-specification following *in vivo* retroviral expression of *Neurog2*

(A) The experimental design involved injecting the RV-CAG-*Neurog2*-IRES-*dsRed* retrovirus into the RMS elbow.

(B) A sagittal view of the adult mouse olfactory bulb (OB) revealed transduced cells (red) following retrovirus injection into the RMS elbow when analyzed at 7 DPT. Transduced neurons could be observed across the OB.

(C–G) Micrographs show that transduced cells lacked TBR1 expression (green) in both the dorsal (C) and ventral (D) areas of the granule cell layer (GCL) and also in the RMS (E), as opposed to preexisting non-transduced glutamatergic neurons in other areas (G).

(H) Histogram showing the number of dsRed-positive transduced cells in the RMS and OB at 7 DPT.

Error bars indicate mean ± SD, n = 3/mice group, t test. Scale bars: 100 μm (B) and 50 μm (C–E).

of an ice-cold medium consisting of 4% bovine serum albumin (BSA; Sigma-Aldrich) in Earle's balanced salt solution (EBSS; Invitrogen) buffered with 20 mM HEPES (Invitrogen) was added in order to stop dissociation. Cells were then centrifuged at 200 × g for 5 min, re-suspended in ice-cold medium consisting of 0.9 M sucrose (Sigma-Aldrich) in 0.5× HBSS, and centrifuged for 10 min at 750 × *g*. The cell pellet was re-suspended in 2 mL ice-cold medium consisting of 4% BSA in EBSS buffered with 2 mM HEPES, and the cell suspension was placed on top of 12 mL of the same medium and centrifuged for 7 min at 200 × *g*. The resulting cell pellet was re-suspended in DMEM/F12 Glutamax (Invitrogen) supplemented with B27 (Invitrogen), 2 mM glutamine (Sigma-Aldrich), 100 units/mL penicillin (Invitrogen), 100 μg/mL streptomycin (Invitrogen), buffered with 8 mM HEPES. Finally, cells were plated on poly-d-lysine (Sigma-Aldrich) coated coverslips at a density of 200–300 cells/mm^2, and after 2 h to allow settlement of the cells, cultures were treated with retroviral or lentiviral vectors for transduction.

Viral vector injections

Stereotactic injections of retrovirus and lentivirus were performed in 2- to 3-month-old C57BL/6 male mice (*Mus musculus*). Prior to stereotactic injections, mice were anesthetized using ketamine (100 mg/kg; CP-Pharma) and xylazine (5 mg/kg; Rompun; Bayer) and placed into a stereotaxic frame. Approximately, 0.5 μL viral suspension was injected using a pulled-glass capillary at the following coordinates (relative to bregma) to target the SEZ: 0.7 (anteroposterior), 1.2 (mediolateral), and 2.1–1.7 (dorsoventral). For transsynaptic tracing experiments, 0.4 μL RABV was injected in the striatum close to the initial retroviral injection in the SEZ (to target primarily transduced cells, particularly *Neurog2*-programmed cells that settled in the striatum) at the following coordinates: 0.8 (anteroposterior), 1.3 (mediolateral), and 2.1–1.7 (dorsoventral).

Sample processing for immunohistochemistry

Mice were deeply anesthetized and then perfused transcardially with saline (0.9%), followed by 4% paraformaldehyde (PFA; P6148; Sigma-Aldrich) (w/v) for 30 min. After this initial fixation, brains were dissected and post-fixed for at least 2 h in 4% PFA. Sagittal brain sections were prepared at a thickness of 50 μm. For detailed immunohistochemistry and immunocytochemistry protocols, see supplemental information.

Electrophysiology

Perforated patch-clamp recordings were performed as previously described (Heinrich et al., 2011).

Image acquisition for quantitative analysis

Images stacks were acquired using an Olympus FV1000 (equipped with 10×/0.4 N.A. air, 20×/0.8 N.A., and 60×/1.42 N.A. oil-immersion objectives) or a Leica TCS SP5 (equipped with a 20×/0.7 N.A. dry objective; Institute of Molecular Biology, Mainz, Germany) confocal microscope or an epifluorescence microscope (Zeiss Axio Imager.M2 equipped with an ApoTome equipped with 20×/0.7 N.A. dry objective). For additional information on the quantification and analysis procedures, please refer to supplemental information.

SUPPLEMENTAL INFORMATION

Supplemental information can be found online at https://doi.org/10.1016/j.stemcr.2023.10.019.

ACKNOWLEDGMENTS

We are grateful to Ana Beltrán-Arranz and Laia Torres-Masjoan for help with monosynaptic tracing experiments. We are grateful to Dr. Magdalena Götz for support throughout the project. We acknowledge the Microscopy Core Facility of the Institute of Molecular Biology (IMB) in Mainz. This work was supported by a grant from the Wellcome Trust (206410/Z/17/Z). For the purpose of open access, the authors have applied a CC BY public copyright license to any author-accepted manuscript version arising from this submission. Furthermore, this work was supported by grants from the Deutsche Forschungsgemeinschaft to B.B. (CRC1080, project number 221828878; BE 4182 11-1, project number 357058359) and to M.S.B. (LE 4610 1, project number 450131873); the Research Initiative of the State of Rhineland-Palatinate at the Johannes Gutenberg University Mainz (ReALity) to B.B.; the Spanish Ministry of Science and Innovation (MICINN) to S.G. (grants RTI2018-099345-B-I00 and PID2021-128796OB-I00) and F.O. (PID2019-109155RB-I00 and BFU2015-70067REDC); and the Inneruniversitäre Forschungsförderung Stufe 1 of the Universitätsmedizin Mainz to S.P. N.M. was supported by a fellowship from the Human Frontiers Science Program (LT000646/2015), W.F. by a fellowship from the China Scholarship Council, J.S.-L. by a fellowship from the UCM-Santander (CT82/20-CT83/20), and S.G. by the Ramón y Cajal Programme (RYC-2015-19185).

AUTHOR CONTRIBUTIONS

S.P., L.M.M. and M.S.B. designed and performed experiments, interpreted and analyzed results, and wrote the manuscript. F.O., M.K., N.M., and W.F. designed and performed experiments. A.G. and K.-K.C. provided essential reagents. S.G. conceptualized, designed, and performed experiments; interpreted and analyzed results; and wrote the manuscript. B.B. conceptualized the study and experiments, interpreted results, and wrote the manuscript. All authors discussed the manuscript.

DECLARATION OF INTERESTS

The authors declare no competing interests.

Received: August 21, 2021
Revised: October 26, 2023
Accepted: October 27, 2023
Published: November 22, 2023

REFERENCES

Amamoto, R., and Arlotta, P. (2014). Development-inspired reprogramming of the mammalian central nervous system. Science *343*, 1239882. https://doi.org/10.1126/science.1239882.

Arlotta, P., and Berninger, B. (2014). Brains in metamorphosis: reprogramming cell identity within the central nervous system. Curr. Opin. Neurobiol. *27*, 208–214. https://doi.org/10.1016/j.conb.2014.04.007.

Azim, K., Hurtado-Chong, A., Fischer, B., Kumar, N., Zweifel, S., Taylor, V., and Raineteau, O. (2015). Transcriptional Hallmarks of Heterogeneous Neural Stem Cell Niches of the Subventricular Zone. Stem Cell. *33*, 2232–2242. https://doi.org/10.1002/stem.2017.

Baser, A., Skabkin, M., Kleber, S., Dang, Y., Gülcüler Balta, G.S., Kalamakis, G., Göpferich, M., Ibañez, D.C., Schefzik, R., Lopez, A.S., et al. (2019). Onset of differentiation is post-transcriptionally controlled in adult neural stem cells. Nature *566*, 100–104. https://doi.org/10.1038/s41586-019-0888-x.

Baumann, V., Wiesbeck, M., Breunig, C.T., Braun, J.M., Köferle, A., Ninkovic, J., Götz, M., and Stricker, S.H. (2019). Targeted removal of epigenetic barriers during transcriptional reprogramming. Nat. Commun. *10*, 2119. https://doi.org/10.1038/s41467-019-10146-8.

Benraiss, A., Toner, M.J., Xu, Q., Bruel-Jungerman, E., Rogers, E.H., Wang, F., Economides, A.N., Davidson, B.L., Kageyama, R., Nedergaard, M., and Goldman, S.A. (2013). Sustained mobilization of endogenous neural progenitors delays disease progression in a transgenic model of Huntington's disease. Cell Stem Cell *12*, 787–799. https://doi.org/10.1016/j.stem.2013.04.014.

Bergami, M. (2015). Experience-dependent plasticity of adult-born neuron connectivity. Commun. Integr. Biol. *8*, e1038444. https://doi.org/10.1080/19420889.2015.1038444.

Berninger, B., Costa, M.R., Koch, U., Schroeder, T., Sutor, B., Grothe, B., and Götz, M. (2007a). Functional properties of neurons derived from *in vitro* reprogrammed postnatal astroglia. J. Neurosci. *27*, 8654–8664. https://doi.org/10.1523/JNEUROSCI.1615-07.2007.

Berninger, B., Guillemot, F., and Götz, M. (2007b). Directing neurotransmitter identity of neurones derived from expanded adult neural stem cells. Eur. J. Neurosci. *25*, 2581–2590. https://doi.org/10.1111/j.1460-9568.2007.05509.x.

Brill, M.S., Ninkovic, J., Winpenny, E., Hodge, R.D., Ozen, I., Yang, R., Lepier, A., Gascón, S., Erdelyi, F., Szabo, G., et al. (2009). Adult generation of glutamatergic olfactory bulb interneurons. Nat. Neurosci. *12*, 1524–1533. https://doi.org/10.1038/nn.2416.

Brill, M.S., Snapyan, M., Wohlfrom, H., Ninkovic, J., Jawerka, M., Mastick, G.S., Ashery-Padan, R., Saghatelyan, A., Berninger, B., and Götz, M. (2008). A dlx2- and pax6-dependent transcriptional code for periglomerular neuron specification in the adult olfactory bulb. J. Neurosci. *28*, 6439–6452. https://doi.org/10.1523/JNEUROSCI.0700-08.2008.

Cebrian Silla, A., Nascimento, M.A., Redmond, S.A., Mansky, B., Wu, D., Obernier, K., Romero Rodriguez, R., Gonzalez Granero, S., García-Verdugo, J.M., Lim, D.A., and Álvarez-Buylla, A. (2021). Single-cell analysis of the ventricular-subventricular zone reveals signatures of dorsal & ventral adult neurogenesis. Elife *10*, e67436. https://doi.org/10.7554/eLife.67436.

Chen, X., Lepier, A., Berninger, B., Tolkovsky, A.M., and Herbert, J. (2012). Cultured subventricular zone progenitor cells transduced with neurogenin-2 become mature glutamatergic neurons and integrate into the dentate gyrus. PLoS One *7*, e31547. https://doi.org/10.1371/journal.pone.0031547.

Costa, M.R., Ortega, F., Brill, M.S., Beckervordersandforth, R., Petrone, C., Schroeder, T., Götz, M., and Berninger, B. (2011). Continuous live imaging of adult neural stem cell division and lineage progression *in vitro*. Development *138*, 1057–1068. https://doi.org/10.1242/dev.061663.

Delgado, A.C., Maldonado-Soto, A.R., Silva-Vargas, V., Mizrak, D., von Känel, T., Tan, K.R., Paul, A., Madar, A., Cuervo, H., Kitajewski, J., et al. (2021). Release of stem cells from quiescence reveals gliogenic domains in the adult mouse brain. Science *372*, 1205–1209. https://doi.org/10.1126/science.abg8467.

Dennis, D.J., Han, S., and Schuurmans, C. (2019). bHLH transcription factors in neural development, disease, and reprogramming. Brain Res. *1705*, 48–65. https://doi.org/10.1016/j.brainres.2018.03.013.

Dennis, D.J., Wilkinson, G., Li, S., Dixit, R., Adnani, L., Balakrishnan, A., Han, S., Kovach, C., Gruenig, N., Kurrasch, D.M., et al. (2017). Neurog2 and Ascl1 together regulate a postmitotic derepression circuit to govern laminar fate specification in the murine neocortex. Proc. Natl. Acad. Sci. USA *114*, E4934–E4943. https://doi.org/10.1073/pnas.1701495114.

Deshpande, A., Bergami, M., Ghanem, A., Conzelmann, K.K., Lepier, A., Götz, M., and Berninger, B. (2013). Retrograde monosynaptic tracing reveals the temporal evolution of inputs onto new neurons in the adult dentate gyrus and olfactory bulb. Proc. Natl. Acad. Sci. USA *110*, E1152–E1161. https://doi.org/10.1073/pnas.1218991110.

Doetsch, F., Caillé, I., Lim, D.A., García-Verdugo, J.M., and Alvarez-Buylla, A. (1999). Subventricular zone astrocytes are neural stem cells in the adult mammalian brain. Cell *97*, 703–716.

Doetsch, F., Petreanu, L., Caille, I., Garcia-Verdugo, J.M., and Alvarez-Buylla, A. (2002). EGF converts transit-amplifying neurogenic precursors in the adult brain into multipotent stem cells. Neuron *36*, 1021–1034.

Dorst, M.C., Díaz-Moreno, M., Dias, D.O., Guimarães, E.L., Holl, D., Kalkitsas, J., Silberberg, G., and Göritz, C. (2021). Astrocyte-derived neurons provide excitatory input to the adult striatal circuitry. Proc. Natl. Acad. Sci. USA *118*, e2104119118. https://doi.org/10.1073/pnas.2104119118.

Felske, T., Tocco, C., Péron, S., Harb, K., Alfano, C., Galante, C., Berninger, B., and Studer, M. (2023). Lmo4 synergizes with Fezf2 to promote direct *in vivo* reprogramming of upper layer cortical neurons and cortical glia towards deep-layer neuron identities. PLoS Biol. *21*, e3002237. https://doi.org/10.1371/journal.pbio.3002237.

Fode, C., Ma, Q., Casarosa, S., Ang, S.L., Anderson, D.J., and Guillemot, F. (2000). A role for neural determination genes in specifying the dorsoventral identity of telencephalic neurons. Genes Dev. *14*, 67–80.

Gabay, L., Lowell, S., Rubin, L.L., and Anderson, D.J. (2003). Deregulation of dorsoventral patterning by FGF confers trilineage differentiation capacity on CNS stem cells *in vitro*. Neuron *40*, 485–499.

Gage, F.H., and Temple, S. (2013). Neural stem cells: generating and regenerating the brain. Neuron *80*, 588–601. https://doi.org/10.1016/j.neuron.2013.10.037.

Garcia, A.D., Doan, N.B., Imura, T., and Bush, T.G. (2004). Sofroniew MV. GFAP-expressing progenitors are the principal source of constitutive neurogenesis in adult mouse forebrain. Nat. Neurosci. *7*, 1233–1241.

Gascón, S., Murenu, E., Masserdotti, G., Ortega, F., Russo, G.L., Petrik, D., Deshpande, A., Heinrich, C., Karow, M., Robertson, S.P., et al. (2016). Identification and Successful Negotiation of a Metabolic Checkpoint in Direct Neuronal Reprogramming. Cell Stem Cell *18*, 396–409. https://doi.org/10.1016/j.stem.2015.12.003.

Gascón, S., Paez-Gomez, J.A., Díaz-Guerra, M., Scheiffele, P., and Scholl, F.G. (2008). Dual-promoter lentiviral vectors for constitutive and regulated gene expression in neurons. J. Neurosci. Methods *168*, 104–112. https://doi.org/10.1016/j.jneumeth.2007.09.023.

Hack, M.A., Saghatelyan, A., de Chevigny, A., Pfeifer, A., Ashery-Padan, R., Lledo, P.M., and Götz, M. (2005). Neuronal fate determinants of adult olfactory bulb neurogenesis. Nat. Neurosci. *8*, 865–872. https://doi.org/10.1038/nn1479.

Hack, M.A., Sugimori, M., Lundberg, C., Nakafuku, M., and Götz, M. (2004). Regionalization and fate specification in neurospheres: the role of Olig2 and Pax6. Mol. Cell. Neurosci. *25*, 664–678. https://doi.org/10.1016/j.mcn.2003.12.012.

Heinrich, C., Blum, R., Gascón, S., Masserdotti, G., Tripathi, P., Sánchez, R., Tiedt, S., Schroeder, T., Götz, M., and Berninger, B. (2010). Directing astroglia from the cerebral cortex into subtype specific functional neurons. PLoS Biol. *8*, e1000373. https://doi.org/10.1371/journal.pbio.1000373.

Heinrich, C., Gascón, S., Masserdotti, G., Lepier, A., Sanchez, R., Simon-Ebert, T., Schroeder, T., Götz, M., and Berninger, B. (2011). Generation of subtype-specific neurons from postnatal astroglia of the mouse cerebral cortex. Nat. Protoc. *6*, 214–228. https://doi.org/10.1038/nprot.2010.188.

Herrero-Navarro, Á., Puche-Aroca, L., Moreno-Juan, V., Sempere-Ferràndez, A., Espinosa, A., Susín, R., Torres-Masjoan, L., Leyva-Díaz, E., Karow, M., Figueres-Oñate, M., et al. (2021). Astrocytes and neurons share region-specific transcriptional signatures that confer regional identity to neuronal reprogramming. Sci. Adv. *7*, eabe8978. https://doi.org/10.1126/sciadv.abe8978.

Hevner, R.F., Hodge, R.D., Daza, R.A.M., and Englund, C. (2006). Transcription factors in glutamatergic neurogenesis: conserved programs in neocortex, cerebellum, and adult hippocampus. Neurosci. Res. *55*, 223–233. https://doi.org/10.1016/j.neures.2006.03.004.

Kovach, C., Dixit, R., Li, S., Mattar, P., Wilkinson, G., Elsen, G.E., Kurrasch, D.M., Hevner, R.F., and Schuurmans, C. (2013). Neurog2 simultaneously activates and represses alternative gene expression programs in the developing neocortex. Cerebr. Cortex *23*, 1884–1900. https://doi.org/10.1093/cercor/bhs176.

Li, S., Mattar, P., Zinyk, D., Singh, K., Chaturvedi, C.P., Kovach, C., Dixit, R., Kurrasch, D.M., Ma, Y.C., Chan, J.A., et al. (2012). GSK3 temporally regulates neurogenin 2 proneural activity in the neocortex. J. Neurosci. *32*, 7791–7805. https://doi.org/10.1523/JNEUROSCI.1309-12.2012.

Lim, D.A., and Alvarez-Buylla, A. (2014). Adult neural stem cells stake their ground. Trends Neurosci. *37*, 563–571. https://doi.org/10.1016/j.tins.2014.08.006.

Llorens-Bobadilla, E., Zhao, S., Baser, A., Saiz-Castro, G., Zwadlo, K., and Martin-Villalba, A. (2015). Single-Cell Transcriptomics Reveals a Population of Dormant Neural Stem Cells that Become Activated upon Brain Injury. Cell Stem Cell *17*, 329–340. https://doi.org/10.1016/j.stem.2015.07.002.

Lois, C., García-Verdugo, J.M., and Alvarez-Buylla, A. (1996). Chain migration of neuronal precursors. Science *271*, 978–981.

Merkle, F.T., Fuentealba, L.C., Sanders, T.A., Magno, L., Kessaris, N., and Alvarez-Buylla, A. (2014). Adult neural stem cells in distinct microdomains generate previously unknown interneuron types. Nat. Neurosci. *17*, 207–214. https://doi.org/10.1038/nn.3610.

Merkle, F.T., Mirzadeh, Z., and Alvarez-Buylla, A. (2007). Mosaic organization of neural stem cells in the adult brain. Science *317*, 381–384. https://doi.org/10.1126/science.1144914.

Mizrak, D., Levitin, H.M., Delgado, A.C., Crotet, V., Yuan, J., Chaker, Z., Silva-Vargas, V., Sims, P.A., and Doetsch, F. (2019). Single-Cell Analysis of Regional Differences in Adult V-SVZ Neural Stem Cell Lineages. Cell Rep. *26*, 394–406.e5. https://doi.org/10.1016/j.celrep.2018.12.044.

Molyneaux, B.J., Arlotta, P., Hirata, T., Hibi, M., and Macklis, J.D. (2005). Fezl is required for the birth and specification of corticospinal motor neurons. Neuron *47*, 817–831. https://doi.org/10.1016/j.neuron.2005.08.030.

Obernier, K., and Alvarez-Buylla, A. (2019). Neural stem cells: origin, heterogeneity and regulation in the adult mammalian brain. Development *146*, dev156059. https://doi.org/10.1242/dev.156059.

Ochiai, W., Nakatani, S., Takahara, T., Kainuma, M., Masaoka, M., Minobe, S., Namihira, M., Nakashima, K., Sakakibara, A., Ogawa, M., and Miyata, T. (2009). Periventricular notch activation and asymmetric Ngn2 and Tbr2 expression in pair-generated neocortical daughter cells. Mol. Cell. Neurosci. *40*, 225–233. https://doi.org/10.1016/j.mcn.2008.10.007.

Ortega, F., Costa, M.R., Simon-Ebert, T., Schroeder, T., Götz, M., and Berninger, B. (2011). Using an adherent cell culture of the mouse subependymal zone to study the behavior of adult neural stem cells on a single-cell level. Nat. Protoc. *6*, 1847–1859. https://doi.org/10.1038/nprot.2011.404.

Ortega, F., Gascón, S., Masserdotti, G., Deshpande, A., Simon, C., Fischer, J., Dimou, L., Chichung Lie, D., Schroeder, T., and Berninger, B. (2013). Oligodendrogliogenic and neurogenic adult subependymal zone neural stem cells constitute distinct lineages and exhibit differential responsiveness to Wnt signalling. Nat. Cell Biol. *15*, 602–613. https://doi.org/10.1038/ncb2736.

Quan, X.J., Yuan, L., Tiberi, L., Claeys, A., De Geest, N., Yan, J., van der Kant, R., Xie, W.R., Klisch, T.J., Shymkowitz, J., et al. (2016). Post-translational Control of the Temporal Dynamics of Transcription Factor Activity Regulates Neurogenesis. Cell *164*, 460–475. https://doi.org/10.1016/j.cell.2015.12.048.

Rogelius, N., Hebsgaard, J.B., Lundberg, C., and Parmar, M. (2008). Reprogramming of neonatal SVZ progenitors by islet-1 and neurogenin-2. Mol. Cell. Neurosci. *38*, 453–459. https://doi.org/10.1016/j.mcn.2008.04.008.

Rouaux, C., and Arlotta, P. (2010). Fezf2 directs the differentiation of corticofugal neurons from striatal progenitors *in vivo*. Nat. Neurosci. *13*, 1345–1347. https://doi.org/10.1038/nn.2658.

Rouaux, C., and Arlotta, P. (2013). Direct lineage reprogramming of post-mitotic callosal neurons into corticofugal neurons *in vivo*. Nat. Cell Biol. *15*, 214–221. https://doi.org/10.1038/ncb2660.

Saghatelyan, A., de Chevigny, A., Schachner, M., and Lledo, P.M. (2004). Tenascin-R mediates activity-dependent recruitment of neuroblasts in the adult mouse forebrain. Nat. Neurosci. *7*, 347–356. https://doi.org/10.1038/nn1211.

Sequerra, E.B. (2014). Subventricular zone progenitors in time and space: generating neuronal diversity. Front. Cell. Neurosci. *8*, 434. https://doi.org/10.3389/fncel.2014.00434.

Wickersham, I.R., Lyon, D.C., Barnard, R.J.O., Mori, T., Finke, S., Conzelmann, K.K., Young, J.A.T., and Callaway, E.M. (2007). Monosynaptic restriction of transsynaptic tracing from single, genetically targeted neurons. Neuron *53*, 639–647. https://doi.org/10.1016/j.neuron.2007.01.033.

Zuccotti, A., Le Magueresse, C., Chen, M., Neitz, A., and Monyer, H. (2014). The transcription factor Fezf2 directs the differentiation of neural stem cells in the subventricular zone toward a cortical phenotype. Proc. Natl. Acad. Sci. USA *111*, 10726–10731. https://doi.org/10.1073/pnas.1320290111.